Journal of Materials Chemistry A

Accepted Manuscript

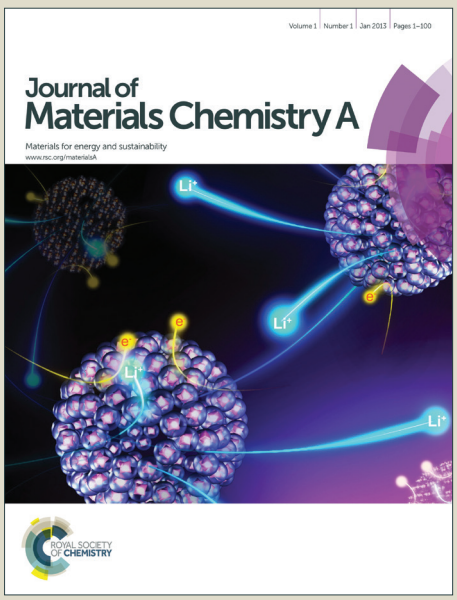

This is an *Accepted Manuscript*, which has been through the Royal Society of Chemistry peer review process and has been accepted for publication.

Accepted Manuscripts are published online shortly after acceptance, before technical editing, formatting and proof reading. Using this free service, authors can make their results available to the community, in citable form, before we publish the edited article. We will replace this *Accepted Manuscript* with the edited and formatted *Advance Article* as soon as it is available.

You can find more information about *Accepted Manuscripts* in the Information for Authors.

Please note that technical editing may introduce minor changes to the text and/or graphics, which may alter content. The journal's standard Terms & Conditions and the Ethical guidelines still apply. In no event shall the Royal Society of Chemistry be held responsible for any errors or omissions in this *Accepted Manuscript* or any consequences arising from the use of any information it contains.

ROYAL SOCIETY OF CHEMISTRY

www.rsc.org/materialsA

Journal Name

COMMUNICATION

Pt-Co Secondary Solid Solution Nanocrystals Supported on Carbon as Next-Generation Catalysts for Oxygen Reduction Reaction

Received 00th January 20xx,
Accepted 00th January 20xx

DOI: 10.1039/x0xx00000x

www.rsc.org/

Yige Zhao, Jingjun Liu*, Yanhui Zhao, Feng Wang* and Ye Song

A novel class of Pt-Co secondary solid solution catalysts with long-range ordered intermetallic $CoPt_3$ as solvent and Co as solute for the oxygen reduction reaction (ORR) is proposed. The catalysts exhibit a volcano-type dependence on Co solid solubility in ORR activity and the optimum catalyst with 10% Co solid solubility shows remarkably enhanced catalytic activity and durability, which can be ascribed to the unique electronic structure of the secondary solid solution catalyst.

The slow kinetics of oxygen reduction reaction (ORR) has been one of the major obstacles for renewable source applications like automotive fuel cells and metal-air batteries.[1-2] Therefore it is of great importance to develop more efficient catalysts than commercial Pt/C catalyst (E-TEK) in consideration of its high cost and poor stability.[3-5] To date, great progress has been made on platinum-based primary solid solution alloy (randomly mixed alloys) through Pt alloying with another transition metal, including Co, Ni, Fe, Cr and Cu.[6-15] Among the alloys above, Pt-Co systems have been paid extensive attention on account of their relatively high activity and durability.[16] Although the current Pt-Co alloys may exhibit high activity owing to the alleged ligand effects as a result of Pt d-band centre shift caused by the added element,[17] their stability still remains an intractable problem because of the serious agglomeration and dissolution of catalysts.[18] Recently, Pt-based intermetallic compounds have attracted much interest for their fixed composition and ordered structure, as they can supply divinable control over geometric and electronic effects not offered by the common random alloys.[19-21] They have been proved to be favorable catalysts with prominent stability and poison tolerance when compared to the conventional primary solid solution alloys.[22-23] Nevertheless, a vital challenge still exists for their practical applications because of the reported low activity.[24] Therefore, synthesizing Pt-based catalysts with concurrently high activity and durability remains a tough problem.

In this regard, the doping of a small number of Co atoms into ordered intermetallic $CoPt_3$ lattice, which has barely been researched, may be a promising strategy to obtain a desired catalyst with both high activity and durability, through forming a new type of secondary solid solution alloy with $CoPt_3$ intermetallic as solvent and Co as solute. As the ORR activity is sensitive to composition, geometrical and electronic structures,[25-26] the added Co atoms will not only significantly improve activity by regulating $CoPt_3$ structure but also maintain its stability by not drastically destroying the long-range order structure with strong covalent bonds, which restricts the secondary component leaching away from the surface and decreases the activity loss.[27] The impact of Co atoms may be embodied in the following aspects. Firstly, the integrated Co atoms may decrease the Pt–Pt distance (ensemble/geometric effect) in $CoPt_3$, which facilitates the valid adsorption of active oxygen and improves the ORR kinetics.[28] Secondly, the incorporation of Co atoms may conduce to forming an unique electronic structure owning higher 5d orbital vacancies, resulting in more π electron transfer from oxygen to Pt surface (ligand/electronic effect) and the downshifting of Pt d-band centre, which promotes ORR activity accordingly. Thus, through exploring the influence of Co solid solubility in the intermetallic on its catalytic performance, developing novel secondary solid solution alloys is a worthwhile research to fabricate next-generation catalysts for the ORR.

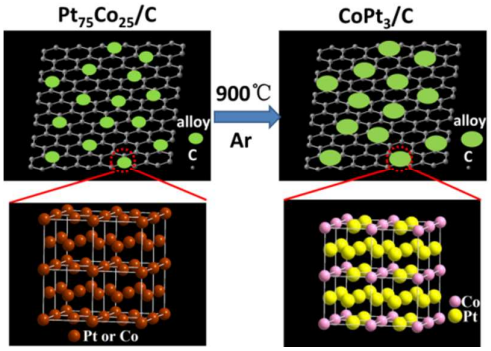

State Key Laboratory of Chemical Resource Engineering, Beijing Key Laboratory of Electrochemical Process and Technology for Materials, Beijing University of Chemical Technology, Beijing 100029, China.
Email: liujingjun@mail.buct.edu.cn (J. Liu); wangf@mail.buct.edu.cn (F. Wang);
Electronic Supplementary Information (ESI) available: detailed experimental procedures, STEM image. See DOI: 10.1039/x0xx00000x

This journal is © The Royal Society of Chemistry 20xx

Please do not adjust margins

Journal of Materials Chemistry A Accepted Manuscript

Scheme 1. The synthesis of intermetallic $CoPt_3$

Following the same thoughts, herein, we report such a novel sort of secondary solid solution nanocrystals via heat treatment of their primary solid solution supported on carbon black. Before fabricating the ultimate secondary solid solution alloys, the ordered intermetallic $CoPt_3$ was first synthesized to serve as a reference catalyst, as depicted as Scheme 1. Figure 1A shows that the as-synthesized alloy particles with narrow size range are uniformly dispersed on the carbon surface and the mean grain size, estimated from a representative particle in the inset high-resolution transmission electron microscope (HRTEM) image, is about 5.8 nm. As depicted from the X-ray diffraction (XRD) spectra of the as-synthesized $CoPt_3$ particles on carbon in Figure 1B, except for the carbon support peak at around 25°, the other peaks correspond to the (100), (110), (111), (200), (210), (211), (220), (300), (310) , (311) and (222) planes of intermetallic $CoPt_3$ with $L1_2$ super-lattice structure. These resulting diffraction peaks are different from those of the corresponding $Pt_{75}Co_{25}$ random alloy having a face-centred cubic (fcc) structure shown in Figure 1B. It implies the formation of intermetallic $CoPt_3$ phase with the super-lattice. This conclusion can be further confirmed by the acquired high-angle annular dark field (HAADF) picture of a single nanoparticle from a fifth-order aberration corrected scanning transmission electron microscopy (STEM), as described in Figure 1C. Because of the Z-contrast of materials,[29] the intensity for different atoms is in proportion to the square of atomic number, making Pt atoms show higher brightness than Co atoms. Owing to the subtle brightness distinction between Pt atoms and Co atoms in Figure 1C, the partial enlarged drawing of a selected region is provided, as shown in Figure 1D. Along the [001] zone axis, the projective $L1_2$ unit cell consists of a periodic square array of Co columns surrounded by Pt columns all around. This is different from the randomly mixed alloy, whose all columns have equal intensity and brightness (Figure S1). Moreover, the $CoPt_3$ (110) lattice plane (d=0.27nm) can be easily recognized from Figure 1D, which further verifies the formation of $CoPt_3$ intermetallic.

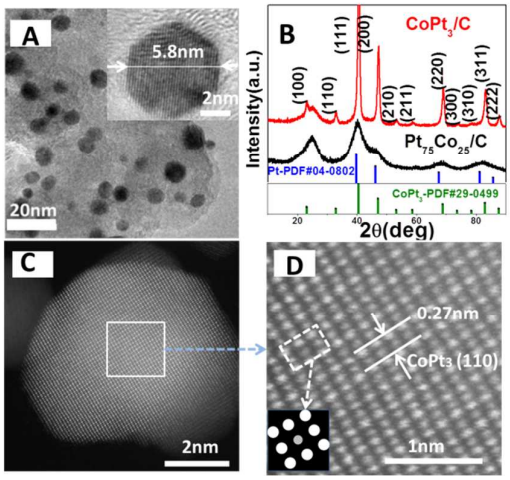

Figure 1. (A) TEM images of $CoPt_3$/C (Insert: HRTEM images); (B) XRD patterns of $Pt_{75}Co_{25}$/C (black curve) and $CoPt_3$/C (red curve). The blue and green vertical lines represent the peak locations of Pt (PDF#04-0802) and intermetallic $CoPt_3$ reflections (PDF#29-0499), respectively; (C) HAADF-STEM image of $CoPt_3$; (D) The partial enlarged drawing of the selected region in C (Insert: the sketch map of $L1_2$ unit cell along the [001] zone axis).

Subsequently, to gain the secondary solid solution alloys based on intermetallic $CoPt_3$, the same heat-treatment method was applied for a wide range of randomly mixed alloy samples with the composition of $Pt_{74}Co_{26}$, $Pt_{72}Co_{28}$, $Pt_{68}Co_{32}$ and $Pt_{64}Co_{36}$, whose compositions were obtained by inductively coupled plasma mass spectrometry (ICP-MS). The catalysts after thermal treatment were characterized with XRD, as shown in Figure 2A, and also display $CoPt_3$ ($L1_2$) super-lattice features. However, these peak locations are slightly shifted to higher angles compared with pure intermetallic $CoPt_3$ phase, indicating that Co is incorporated into $CoPt_3$ lattice to form a secondary solid solution phase with a concomitant lattice contraction. Moreover, these peaks move along higher angle direction with the increase of Co content, revealing that the Co solid solubility increases accordingly. Thus, based on Co solid solubility in the intermetallic $CoPt_3$ phase, these secondary solid solution catalysts can be marked by Co-1%, Co-4%, Co-10% and Co-15% (atom fraction of doped Co elements), respectively. The positions of added Co atoms were explored through evaluating the atomic-level scattering of Pt and Co atoms in the nanoparticles on an energy-dispersive X-ray (EDX) equipped in STEM, which are shown in Figure 2(B-D). The Pt (green) versus Co (red) image (Figure 2E) shows the uniform distribution of Pt and Co elements, which suggests Co atoms are randomly doped into $CoPt_3$ lattice and occupy the sites of part of Pt atoms, as depicted as Figure 2(F).

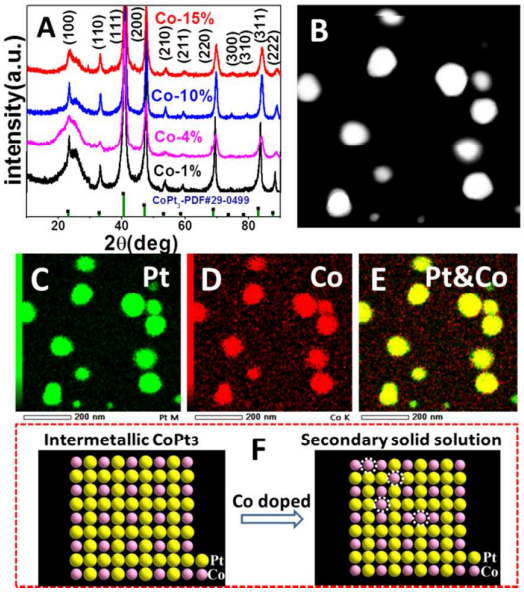

This journal is © The Royal Society of Chemistry 20xx

Please do not adjust margins

Journal of Materials Chemistry A Accepted Manuscript

Figure 2. (A) XRD patterns; (B) ADF-STEM overview image of the Co-10% nanoparticles; (C-E) EDX elementary distribution mapping of (C) Pt, (D) Co and (E) Pt versus Co; (F) The schematic illustration of Co random into the ordered $CoPt_3$. Circled in white are the sites replaced by Co atoms in secondary solid solution.

To confirm that the long-range ordered structure of $CoPt_3$ is not dramatically destroyed after Co doping, the atomic arrangement of the Pt-Co secondary solid solution (Co-10%) was further characterized with STEM and the obtained HAADF image of a single nanoparticle is shown in Figure S2. As observed, the atomic arrangement of the Co-doped $CoPt_3$ is almost similar to that of the pure $CoPt_3$ intermetallic phase shown in Figure 1D. It provides a direct proof that the framework of the $CoPt_3$ was not dramatically destroyed after Co doping. Since regulating the composition and phase structure of catalysts are significant to fine-tuning electronic and geometric effects, which in turn improve their ORR performances, the dependence of catalytic activity on Co solid solubility in $CoPt_3$ phase is worth investigating and will be discussed next.

The correlation between Co solid solubility and ORR activity was systematically researched by rotating disk electrode (RDE) in O_2-saturated 1M NaOH solutions. For comparison, the ordered $CoPt_3$ sample, regarded as 0% Co solid solubility, was also added to the set of study. The obtained ORR polarization curves at 1600rpm with a sweep rate of 5mV/s are shown in Figure 3A. The half-wave potentials ($E_{1/2}$) and kinetics current densities (J_k) at 0.9V versus RHE follow the same order: Co-10%> Co-4%> Co-1%> Pt/C> $CoPt_3$>Co-15% (Figure 3B and C). Interestingly, the ORR activities of secondary solid solution alloys display a volcano type as a function of Co solid solubility, where the peak corresponds to the Co-10% catalyst, which exhibits the most positive potential for $E_{1/2}$ (1.0V), a remarkably positive shift of ~100mV in contrast with Pt/C, and the highest J_k value (15.0mA.cm^{-2}), nearly two times that of commercial Pt/C (7.62mA.cm^{-2}). Moreover, the calculated mass activities of Pt as the function of Co solid solubility were fitted and plotted in Figure 3D. All the catalysts with Co solid solubility from 1 at% to 13 at% display better mass activities than that of Pt/C, and a similar volcano type can be observed. To better understand the observed difference in ORR activity, the specific activities of all the samples were calculated based on Figure S3 and shown in Figure 3E. The results indicate that the analogous volcano type still exists for the different Co solid solution solubility samples and that the optimum Co-10% catalysts(0.34mA/cm^2) exhibits a specific activity of 2.1 times that of the commercial Pt/C(0.16mA/cm^2). These above outcomes illustrate that the ORR activities are strongly dependent on Co solid solubility and that the doping of a small number of Co atoms into $CoPt_3$ plays a significantly positive role in ORR activity enhancement, while excess Co atoms will reduce the activity. Based on the thermal equilibrium phase diagram of Co-Pt binary alloy system[30], we found that the solid solubility of the secondary solid solution based $CoPt_3$ is limited. If excess Co atoms were doped, the high ORR activity of the Pt-Co secondary solid solution catalysts is likely to be decayed dramatically by the chemical precipitation of random Pt-Co binary alloy or other Pt-Co compound. This is why the Co-15% catalyst exhibits poor ORR activity relative to the other Pt-Co secondary solid solution catalysts.

According to previous studies, [31-32] in binary alloys the alloy compositions can alter Pt surface electronic structures, which will have an important influence on their corresponding ORR activities. In our case, the improved ORR activity of the secondary solid solution catalysts may be attributed to the unique electronic interaction as a consequence of Co doped into $CoPt_3$. The nature responsible for ORR activity enhancement will be disclosed by the following electronic parameter analysis.

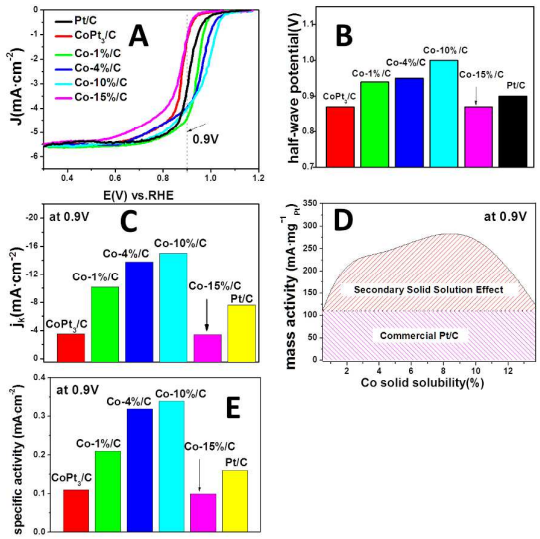

Figure 3. (A) The ORR polarization curves measured at 1600rpm in O_2-saturated 1M NaOH solutions with a sweep rate of 5mV/s in the negative direction; (B) The half-wave potentials; (C) The kinetics current densities; (D) The mass activities of Pt as a function of Co solid solubility. (E) The specific activities for these catalysts.

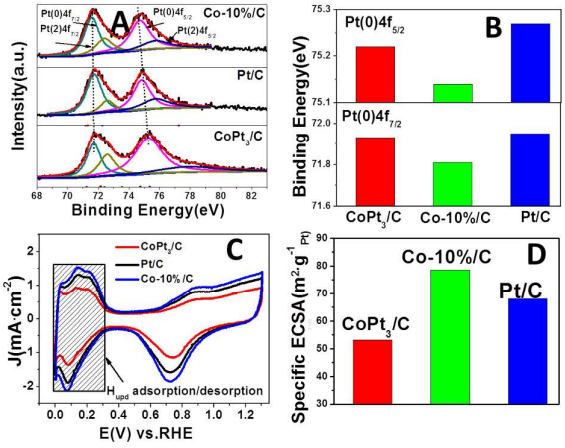

Figure 4. (A) High resolution XPS spectra showing Pt 4f peaks; (B) The fitted Pt(0) $4f_{5/2}$ and Pt(0) $4f_{7/2}$ core-level binding

Journal of Materials Chemistry A Accepted Manuscript

energies; (C) CV curves; (D) The calculated specific ECSA using the data of (C).

Thus, we conducted X-ray photoelectron spectra (XPS) experiments on a representative secondary solid solution (Co-10%), intermetallic $CoPt_3$ and commercial Pt/C, respectively. Considering that the Co 2p peaks are very weak owing to the very low Co solubility in the $CoPt_3$ compound (Figure S4) and that the active sites for the Pt-Co secondary solid solution alloys are Pt atoms rather than Co atoms, the influence of electronic structure will be explained by the analysis of Pt 4f peaks legitimately. The obtained Pt 4f core-level binding energies of these catalysts are described in Figure 4A. It can be seen that Pt exists in diverse valence states like Pt(0) (metallic Pt), Pt(2) (PtO and $Pt(OH)_2$). By the comparison of the relative intensities, we discover that Pt(0) dominates among the above components, as it can afford more appropriate sites for ORR than Pt(2).[33] Thus, We compare the Pt(0) binding energies (including $4f_{5/2}$ and $4f_{7/2}$) among these catalysts (Figure 4B), discovering that Pt 4f peaks of Co-10% shift to lower binding energies in contrast to that of Pt/C catalyst, while Pt 4f peaks of $CoPt_3$/C shift to the opposite direction. It indicates that the electronic structure of Pt is changed by Co atoms doped into $CoPt_3$. Since the modification in the binding energies of core level announces the shift of its d-band centre relative to Fermi level[33-34] and they are deemed to accompany variations in the same direction,[35] the downshift in the Pt 4f binding energy demonstrates the downshift of its d-band centre. In view of the Hammer–Nørskov model,[36-38] the downshifted d-band centre lowers the density of state on the Fermi level and weakens the chemisorption bonds. So the chemical adsorptions of OH_{ads} species on the surface are reduced, which makes for generating more active sites for ORR.[39] Unfortunately, the negative shift of d-band centre can also lower O_2 adsorption strength, then impede O–O bond breaking, finally hamper the ORR kinetics. In our case, the Co-10% catalyst exhibits the most outstanding performance among these catalysts, suggesting that its Pt 4f binding energy has an optimum value to balance the above two opposite impacts. According to the density functional theory (DFT) calculations by former researchers, [40] if a catalyst binds oxygen too strongly, the rate of its ORR will be restricted by the removal of surface oxide. Thus, concerning the $CoPt_3$ intermetallic, owing to the strong ability of binding oxygen arised from the highest binding energy, its activity is limited by the elimination of OH_{ads} species; that is to say, its surface is oxidized and unreactive. In conclusion, the enhanced ORR activity of secondary solid solution alloys primarily roots in the special electronic structure. To confirm this conclusion, the XPS results of these secondary solid solution samples are provided, as shown in Figure S5. It can be seen that the Pt 4f peaks of Co-1%, Co-4%, Co-10% catalysts shift to lower binding energies relative to that of the commercial Pt/C, while the corresponding Pt 4f peak of Co-15% catalyst shift to higher binding energy. In addition, the Co-1%, Co-4%, Co-10% catalysts exhibited better performance than Pt/C, while Co-15% didn't. It supplies another proof that the origin of ORR activity enhancement is strongly related to the unique electronic structure. The electronic effects include electron transfer, changes in hybridization, and changes in the environmental charge density. In our case, because of the relative smaller electronegative difference between Pt and Co atoms in the Pt-Co alloy system than that between metal and nonmetal atoms for metal-nonmetal system (such as Fe_3C), the effects of electron transfer and changes in the environmental charge density are smaller than that of hybridization. Therefore, electronic effect embodied in the change of hybridization, which is induced by Co doped in $CoPt_3$, becomes the main factor resulting in the changes of electronic structures. From the above analysis, we speculate that the unique electronic structures of secondary solid solution nanocrystals, raised by the changes in hybridization of two metals, can help to desorb OH_{ads} species on the surface of the catalysts, which can offer more active sites for the ORR.

To confirm this deduction, cyclic voltammetry (CV) for electrochemical surface area (ECSA) study was conducted in N_2-purged $HClO_4$ (0.1M) solutions at a sweep rate of 50mV/s, as depicted in Figure 4C. The J value was normalized to the geometric area of electrode ($0.247cm^2$). The ECSA values were calculated on the basis of the charge associated with the hydrogen adsorption/desorption region and assuming a factor of $210\mu C/cm^2$ for the adsorption of a hydrogen monolayer.[41] From Figure 4D, we can see that the optimum Co-10% catalyst has the highest ECSA value ($77.6m^2/g$ Pt). It further confirms that the modification of the electronic structures of the secondary solid solution nanocrystal caused by the doping of Co (10%) can effectively remove the OH_{ads} species adsorbed on the surface of the catalyst, which provides more active sites for O_2, leading to the remarkably enhanced ORR activity.

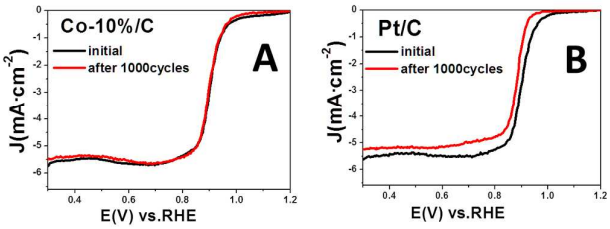

Figure 5. Characterization of stability for ORR: Polarization curves of Co-10% (A) and Pt/C (B) catalysts before and after ADT.

Moreover, the durability of the optimum catalyst (Co-10%) was evaluated by polarization curves before and after accelerated durability test (ADT), as depicted in Figure 5A. The ADT was conducted by potential cycling between 0.167V and 1.267V versus RHE in the O_2-purged 1M NaOH solution at a scan rate of 100mV/s for 1000 cycles. It can be observed that the Co-10% sample shows a degradation of 5mV in its half-wave potential after ADT, in contrast, the corresponding change for Pt/C reaches to 25mV (Figure 5B). The outstanding stability of secondary solid solution catalysts can be ascribed to the well-known stability of $CoPt_3$ intermetallic,[42] because

This journal is © The Royal Society of Chemistry 20xx

Please do not adjust margins

Journal of Materials Chemistry A Accepted Manuscript

few Co atoms doped into $CoPt_3$ will not drastically destroy the long-range order structure with strong covalent bonds, which restricts the secondary component leaching away and decreases the activity loss. To evaluate their practicability of the Pt-Co secondary solid solution nanocrystals in proton exchange membrane fuel cell, the ORR activity and stability (Co-10%) of the catalysts have been performed in 0.1 M $HClO_4$ solution and the obtained results are shown in Figure S6 and Figure S7. The Pt-Co catalyst displays slightly improved ORR activity and stability, compared to that of the commercial Pt/C catalyst, but it don't exhibit remarkable ORR activity enhancement. The relatively low ORR activity of the catalyst may be ascribed to the leaching out of doped Co atoms in $CoPt_3$ compound in acid environments. But, it needs to be further confirmed by future investigation in detail.

In summary, we have fabricated Pt-Co secondary solid solution nanocrystals with long-range ordered $CoPt_3$ intermetallic as solvent and Co as solute. Their ORR activities exhibit volcano-type dependence on Co solid solubility and the best Co-10% secondary solid solution catalyst displays remarkable increase in ORR activity than commercial Pt/C (E-TEK). The observed activity enhancement is strongly dependent on the unique electronic structures, which conduce to more electrochemical active sites and this idea is further proved by CV. Stability tests indicate that the secondary solid solution catalysts are more durable than Pt/C, which can be attributed to the well-known stability of intermetallic, since few Co atoms into $CoPt_3$ will not drastically destroy the long-range order structure. This study may provide a promisingly new idea to synthesize catalysts with both prominent activity and stability, and further supplies reference values for other secondary solid solution catalysts through the doping of transition metal (such as Ni, Fe, Cu, and so on) into their intermetallic.

Acknowledgements

The authors are grateful to the National Natural Science Funds of China for financial support (Grant No. 50972003, 51125007).

Notes and references

1 M. K. Debe, *Nature*, 2012, **486**, 43-51.
2 Y. Liang, H. Wang, P. Diao, W. Chang, G. Hong, Y. Li, M. Gong, L. Xie, J. Zhou and J. Wang, *J. Am. Chem. Soc.*, 2012, **134**, 15849-15857.
3 D. Geng, Y. Chen, Y. Chen, Y. Li, R. Li, X. Sun, S. Ye and S. Knights, *Energy Environ. Sci.*, 2011, **4**, 760-764.
4 J. Duan, Y. Zheng, S. Chen, Y. Tang, M. Jaroniec and S. Qiao, *Chem. Commun.*, 2013, **49**, 7705-7707.
5 W. Song, Z. Chen, C. Yang, Z. Yang, J. Tai, Y. Nan and H. Lu, *J. Mater. Chem. A*, 2015, **3**, 1049-1057.
6 J. Greeley, I. Stephens, A. Bondarenko, T. P. Johansson, H. A. Hansen, T. Jaramillo, J. Rossmeisl, I. Chorkendorff and J. K. Nørskov, *Nat. Chem.*, 2009, **1**, 552-556.
7 V. R. Stamenkovic, B. S. Mun, M. Arenz, K. J. Mayrhofer, C. A. Lucas, G. Wang, P. N. Ross and N. M. Markovic, *Nat. Mater.*, 2007, **6**, 241-247.
8 H. Yano, M. Kataoka, H. Yamashita, H. Uchida and M. Watanabe, *Langmuir*, 2007, **23**, 6438-6445.
9 B. J. Hwang, S. M. S. Kumar, C.-H. Chen, Monalisa, M.-Y. Cheng, D.-G. Liu and J.-F. Lee, *J. Phys. Chem. C*, 2007, **111**, 15267-15276.
10 E. I. Santiago, L. C. Varanda and H. M. Villullas, *J. Phys. Chem. C*, 2007, **111**, 3146-3151.
11 S. Papadimitriou, S. Armyanov, E. Valova, A. Hubin, O. Steenhaut, E. Pavlidou, G. Kokkinidis and S. Sotiropoulos, *J. Phys. Chem. C*, 2010, **114**, 5217-5223.
12 H. L. Xin, S. Alayoglu, R. Tao, A. Genc, C.-M. Wang, L. Kovarik, E. A. Stach, L.-W. Wang, M. Salmeron and G. A. Somorjai, *Nano Lett.*, 2014, **14**, 3203-3207.
13 J. Wu, J. Zhang, Z. Peng, S. Yang, F. T. Wagner and H. Yang, *J. Am. Chem. Soc.*, 2010, **132**, 4984-4985.
14 C. Wang, M. Chi, G. Wang, D. Van der Vliet, D. Li, K. More, H. H. Wang, J. A. Schlueter, N. M. Markovic and V. R. Stamenkovic, *Adv. Funct. Mater.*, 2011, **21**, 147-152.
15 X. Yu, D. Wang, Q. Peng and Y. Li, *Chem. Commun.*, 2011, **47**, 8094-8096.
16 D. Wang, H. L. Xin, R. Hovden, H. Wang, Y. Yu, D. A. Muller, F. J. DiSalvo and H. D. Abruña, *Nat. Mater.*, 2013, **12**, 81-87.
17 M. Bele, P. Jovanovič, A. Pavlišič, B. Jozinović, M. Zorko, A. Rečnik, E. Chernyshova, S. Hočevar, N. Hodnik and M. Gaberšček, *Chem. Commun.*, 2014, **50**, 13124-13126.
18 L. Su, S. Shrestha, Z. Zhang, W. Mustain and Y. Lei, *J. Mater. Chem. A*, 2013, **1**, 12293-12301.
19 Z. Liu, G. S. Jackson and B. W. Eichhorn, *Angew. Chem. Int. Ed.*, 2010, **49**, 3173-3176.
20 T. Ghosh, M. B. Vukmirovic, F. J. DiSalvo and R. R. Adzic, *J. Am. Chem. Soc.*, 2010, **132**, 906-907.
21 X. Ji, K. T. Lee, R. Holden, L. Zhang, J. Zhang, G. A. Botton, M. Couillard and L. F. Nazar, *Nat. Chem.*, 2010, **2**, 286-293.
22 S. Zhang, S. Guo, H. Zhu, D. Su and S. Sun, *J. Am. Chem. Soc.*, 2012, **134**, 5060-5063.
23 H. Chen, D. Wang, Y. Yu, K. A. Newton, D. A. Muller, H. c. Abruña and F. J. DiSalvo, *J. Am. Chem. Soc.*, 2012, **134**, 18453-18459.
24 M. Watanabe, K. Tsurumi, T. Mizukami, T. Nakamura and P. Stonehart, *J. Electrochem. Soc.*, 1994, **141**, 2659-2668.
25 J. Wu, L. Qi, H. You, A. Gross, J. Li and H. Yang, *J. Am. Chem. Soc*, 2012, **134**, 11880-11883.
26 P. Strasser, S. Koh, T. Anniyev, J. Greeley, K. More, C. Yu, Z. Liu, S. Kaya, D. Nordlund and H. Ogasawara, *Nat. Chem.*, 2010, **2**, 454-460.
27 J. K. Nørskov, T. Bligaard, J. Rossmeisl and C. H. Christensen, *Nat. Chem.*, 2009, **1**, 37-46.
28 Z. Duan and G. Wang, *J. Phys. Chem. C*, 2013, **117**, 6284-6292.
29 A. V. Crewe, J. Wall and J. Langmore, *Science*, 1970, **168**, 1338-1340.
30 S. Doi, F. Wang, K. Hosoiri and T. Watanabe, *Mater Trans*, 2003, **44**, 649-652.
31 Y. Zhao, J. Liu, Y. Zhao and F. Wang, *Phys. Chem. Chem. Phys.*, 2014, **16**, 19298-19306.
32 Z. Sun, J. Masa, W. Xia, D. König, A. Ludwig, Z.-A. Li, M. Farle, W. Schuhmann and M. Muhler, *ACS. Catal.*, 2012, **2**, 1647-1653.
33 P. Wu, H. Zhang, Y. Qian, Y. Hu, H. Zhang and C. Cai, *J. Phys. Chem. C*, 2013, **117**, 19091-19100.
34 J. Kitchin, J. K. Nørskov, M. Barteau and J. Chen, *J. Chem. Phys*, 2004, **120**, 10240-10246.
35 M. V. Ganduglia-Pirovano, V. Natoli, M. Cohen, J. Kudrnovský and I. Turek, *Phys. Rev. B*, 1996, **54**, 8892.
36 B. Hammer and J. K. Nørskov, *Adv. Catal.*, 2000, **45**, 71-129.
37 B. Hammer, Y. Morikawa and J. K. Nørskov, *Phys. Rev. Lett.*, 1996, **76**, 2141.
38 A. Ruban, B. Hammer, P. Stoltze, H. L. Skriver and J. K. Nørskov, *J. Mol. Catal. A: Chem.*, 1997, **115**, 421-429.

Journal of Materials Chemistry A Accepted Manuscript

39 K. Zhang, Q. Yue, G. Chen, Y. Zhai, L. Wang, H. Wang, J. Zhao, J. Liu, J. Jia and H. Li, *J. Phys. Chem. C*, 2011, **115**, 379-389.
40 V. Stamenkovic, B. S. Mun, K. J. Mayrhofer, P. N. Ross, N. M. Markovic, J. Rossmeisl, J. Greeley and J. K. Nørskov, *Angew. Chem. Int. Ed.*, 2006, **118**, 2963-2967.
41 K. A. Kuttiyiel, K. Sasaki, Y. Choi, D. Su, P. Liu and R. R. Adzic, *Nano Lett.*, 2012, **12**, 6266-6271.
42 E. V. Shevchenko, D. V. Talapin, H. Schnablegger, A. Kornowski, Ö. Festin, P. Svedlindh, M. Haase and H. Weller, *J. Am. Chem. Soc.*, 2003, **125**, 9090-9101.

Journal of Materials Chemistry A Accepted Manuscript

This journal is © The Royal Society of Chemistry 20xx

Table of Contents

Title: Pt-Co Secondary Solid Solution Nanocrystals Supported on Carbon as Next-Generation Catalysts for Oxygen Reduction Reaction

Yige Zhao, Jingjun Liu*, Yanhui Zhao, Feng Wang*and Ye Song

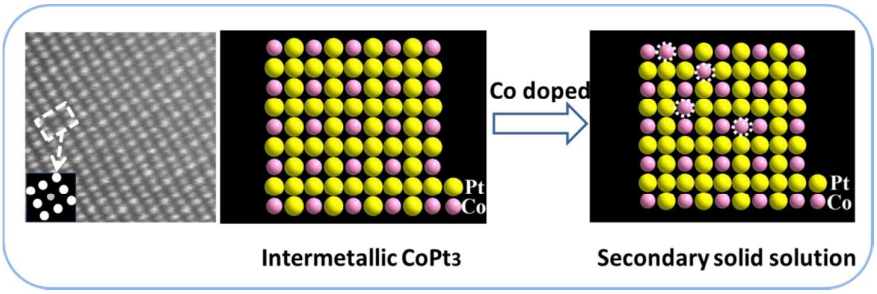

One sentence of text: A secondary solid solution alloy with long-term ordered $L1_2$ $CoPt_3$ intermetallic compound as solvent and Co as solute is proposed.

Journal of Materials Chemistry A Accepted Manuscript